



Experimental mutual coherence from separable coherent qubits

Nikola Horová , Robert Stárek, Michal Mičuda , Jaromír Fiurášek , Michal Kolář , and Radim Filip
Department of Optics, Faculty of Science, Palacký University Olomouc, 17. listopadu 1192/12, Olomouc 77900, Czech Republic

 (Received 5 April 2022; accepted 11 July 2022; published 28 July 2022)

Quantum coherence is a fundamental resource in modern quantum physics with important applications in quantum technologies. In composite quantum systems, various forms of coherence emerge and play an important role, such as the global coherence, coherence of local subsystems, and the recently introduced mutual coherence. We investigate states that maximize the mutual coherence in various subspaces of the overall two-qubit Hilbert space and discover a nontrivial asymmetric optimal state in the three-dimensional subspace. We experimentally generate this optimal state from two factorized photonic qubits by a strictly incoherent probabilistic quantum operation that projects the input state onto the desired three-dimensional subspace. For comparison, we also experimentally test the preparation of states with maximal mutual coherence by unitary transformations of input product states. These proof-of-principle tests demonstrate the initial steps of control of mutual quantum coherence in qubit systems.

DOI: [10.1103/PhysRevA.106.012440](https://doi.org/10.1103/PhysRevA.106.012440)

I. INTRODUCTION

Quantum coherence [1–4] is an indispensable and valuable resource for, e.g., quantum information processing [5] or quantum metrology [6]. Properties and transformations of quantum coherence, as well as coherence distillation under various settings, have been recently investigated in numerous works [7–14]. In a compound quantum system, the coherence can be distributed in diverse and nontrivial ways. Besides the coherence of the *global* state [1], one can consider the *local* coherence of marginal states with respect to local bases. Interestingly, a new form of quantum coherence can be established by the difference of global and local coherences, the so-called *mutual* coherence [15–19]. This quantity characterizes the amount of quantum state coherence that is not contained in the local (marginal) states of the subsystems. From the quantum information perspective, the mutual coherence can be interpreted as the difference in distillable coherence [2,20] of the global state of a compound system and the product of all local states of the subsystems constituting the compound system. Notably, this new form of coherence can also be interpreted as the additional work potentially obtainable in a specific thermodynamic process [21], if global coherence is utilized instead of the sum of local ones. The basis-optimized value of mutual coherence, known as the correlated coherence, characterizes a new type of quantum correlations [18] of the subsystems, which are conceptually different from entanglement or quantum mutual information.

For a pair of d -dimensional quantum systems, the mutual coherence is maximized by a maximally entangled state,

$$|\Psi\rangle = \frac{1}{d} \sum_{j,k=0}^{d-1} e^{\frac{2\pi i j k}{d}} |j\rangle|k\rangle, \quad (1)$$

where $|j\rangle$ denotes the basis of free states with zero coherence. The state $|\Psi\rangle$ exhibits complete symmetry in the sense of

equal probabilities of basis states $|j\rangle|k\rangle$. However, applications may require coherence to be contained in a specific subspace of the full Hilbert space. If we impose a constraint that the state $|\psi\rangle$ can be formed by the superposition of N free product states $|jk\rangle$ only, where $N < d^2$, then the optimal state that maximizes the mutual coherence in such subspace can become nontrivial and not a maximally entangled state. Here we investigate this interesting phenomenon for the simplest nontrivial composite Hilbert space of a pair of qubits ($d = 2$) and $N = 3$. In our study, we quantify the coherence by the relative entropy of coherence, which is a well-behaved additive measure of coherence. We identify the optimal state for the $d = 2$, $N = 3$ setting and find that it exhibits uneven populations of the three basis states and therefore does not represent a state with maximum global coherence in the given subspace of the full Hilbert space. We then generate this optimal state experimentally from easily accessible product state of individual qubits. We aim at preparation of the optimal state by free transformation of the resource theory, namely, by a probabilistic strictly incoherent operation represented by a single Kraus operator diagonal in the basis of free states [9,20]. For comparison, we also test an alternative preparation scheme based on the combination of the quantum controlled- Z gate and a local single-qubit unitary operation that couples the basis states $|0\rangle$ and $|1\rangle$.

Our work reveals that care is needed if one considers transformations of different forms of coherence between each other in a compound system. If one aims to gain maximum mutual coherence, the form shared among subsystems and not present only locally, one cannot directly assume that the optimal state is some globally maximally coherent state. On the contrary, individual cases should be examined separately with caution.

The rest of the paper is organized as follows. In Sec. II, we review the definition of mutual quantum coherence and identify optimal states that maximize the mutual coherence in various subspaces of the two-qubit Hilbert space. The

experimental setup is described in Sec. III, and in Sec. IV, we present and discuss our experimental results. Finally, Sec. V contains a brief summary and conclusions.

II. MUTUAL QUANTUM COHERENCE

Let us start with some definitions. We choose to quantify the coherence of a quantum state $\hat{\rho}$ by the relative entropy of coherence [1],

$$C(\hat{\rho}) = S(\hat{\rho}||\Delta(\hat{\rho})) = S(\Delta(\hat{\rho})) - S(\hat{\rho}), \quad (2)$$

where $S(\hat{\rho}) = -\text{Tr}[\hat{\rho} \log_2 \hat{\rho}]$ is the von Neumann entropy and $\Delta(\hat{\rho}) = \sum_j \rho_{jj} |j\rangle\langle j|$ is the fully dephased state. Mutual coherence of a bipartite system $\hat{\rho}_{AB}$ is then defined as a difference between the coherence of the global state and the local coherences of the two subsystems [15–18, 22–24],

$$C_M(\hat{\rho}_{AB}) = C(\hat{\rho}_{AB}) - C(\hat{\rho}_A) - C(\hat{\rho}_B). \quad (3)$$

Here, $\hat{\rho}_i = \text{Tr}_{j \neq i}(\hat{\rho}_{AB})$ is the density matrix of subsystem i . For the chosen coherence measure (2), it is possible to express the mutual coherence as a difference of relative entropies,

$$C_M(\hat{\rho}_{AB}) = S(\hat{\rho}_{AB}||\hat{\rho}_A \otimes \hat{\rho}_B) - S(\Delta(\hat{\rho}_{AB})||\Delta(\hat{\rho}_A) \otimes \Delta(\hat{\rho}_B)), \quad (4)$$

where $S(\hat{\rho}||\hat{\sigma}) = \text{Tr}(\hat{\rho} \log_2 \hat{\rho}) - \text{Tr}(\hat{\rho} \log_2 \hat{\sigma})$.

The relative entropy of coherence is additive,

$$C(\hat{\rho}_A \otimes \hat{\rho}_B) = C(\hat{\rho}_A) + C(\hat{\rho}_B), \quad (5)$$

which ensures that the mutual coherence vanishes for any product state, $C_M(\hat{\rho}_A \otimes \hat{\rho}_B) = 0$. Note that certain coherence measures do not satisfy the additivity property (5). As an example, take the measure of coherence based on the ℓ_1 norm [3, 25], which is defined as

$$C_{\ell_1}(\hat{\rho}) = \sum_{j \neq k} |\rho_{jk}|,$$

where ρ_{jk} are density matrix elements in the basis of free states with zero coherence. Using the ℓ_1 measure, one gets

$$C_{\ell_1}(\hat{\rho}_A \otimes \hat{\rho}_B) = C_{\ell_1}(\hat{\rho}_A)C_{\ell_1}(\hat{\rho}_B) + C_{\ell_1}(\hat{\rho}_A) + C_{\ell_1}(\hat{\rho}_B).$$

Consequently, this measure can yield a nonzero mutual coherence for a product state,

$$C_{M, \ell_1}(\hat{\rho}_A \otimes \hat{\rho}_B) = C_{\ell_1}(\hat{\rho}_A)C_{\ell_1}(\hat{\rho}_B).$$

We therefore consider additivity to be a natural requirement on a coherence measure that is used to calculate the mutual coherence. For this reason, we have chosen the relative entropy of coherence, which is a widely used measure of coherence with good properties. The relative entropy of coherence has a clear operational interpretation as the distillable coherence and it is also relevant in the context of quantum thermodynamics [21].

The mutual coherence combines together the concepts of coherence and quantum correlations differently from entanglement. Naively, one could conjecture that maximally entangled states maximize the mutual coherence among all pure states in a given considered class. Interestingly, we find that this is not always the case. We focus on a system composed of two qubits and consider pure states that are formed by the superposition of N free basis states $|jk\rangle$, where $j, k \in$

$\{0, 1\}$. For $N = 2$ and $N = 4$, we find that the mutual coherence is indeed maximized for maximally entangled states,

$$|\psi_2\rangle = \frac{1}{\sqrt{2}}(|00\rangle + |11\rangle) \quad (6)$$

and

$$|\psi_4\rangle = \frac{1}{2}(|00\rangle + |01\rangle + |10\rangle - |11\rangle). \quad (7)$$

We have $C_M(\psi_2) = 1$ and $C_M(\psi_4) = 2$, which saturate the bound $C_M = \log_2 N$ on mutual coherence of a pure bipartite state formed by the superposition of N free states $|jk\rangle$. By contrast, for $N = 3$, we found by exhaustive numerical search that the pure state that maximizes C_M is formed by an unbalanced superposition of the three basis states,

$$|\psi_3\rangle = c|11\rangle + \sqrt{\frac{1-c^2}{2}}(|01\rangle + |10\rangle), \quad (8)$$

where $c \approx 0.277$ and $\sqrt{\frac{1-c^2}{2}} \approx 0.679$. For this state, we get $C_M(\psi_3) \approx 1.1$, which exceeds the maximum mutual coherence achievable by the superposition of two free basis states. The most interesting feature of the optimal state $|\psi_3\rangle$ is the strong imbalance in absolute values of probability amplitudes, meaning that this state is *not maximally coherent* in the sense of the ordinary coherence C of the total state. In fact, the maximally coherent [9] analog of $|\psi_3\rangle$, $|\phi_3\rangle = 1/\sqrt{3}(|11\rangle + |10\rangle + |01\rangle)$, exhibits a suboptimal value of the mutual coherence, $C_M \approx 0.85$. The state $|\psi_3\rangle$ can be seen as a superposition of the maximally entangled state $\frac{1}{\sqrt{2}}(|01\rangle + |10\rangle)$ and a product state $|11\rangle$. When we form the linear combination (8) and begin to increase the value of c , we increase the coherence of the total state, but we also introduce nonzero local coherences. While the first effect increases the mutual coherence, the other tends to reduce it, and it turns out that the maximum occurs for a specific unbalanced superposition.

Let us conclude this section by noting that the states $|\psi_j\rangle$ are representatives of whole classes of optimal states because local bit flips $\hat{\sigma}_X = |0\rangle\langle 1| + |1\rangle\langle 0|$ and phase shifts $\exp(i\theta\hat{\sigma}_Z)$, where $\hat{\sigma}_Z = |0\rangle\langle 0| - |1\rangle\langle 1|$, do not change the mutual coherence and also do not change the number of free basis states in the superposition.

III. EXPERIMENT

We next investigate the experimental preparation of the optimal states $|\psi_j\rangle$ from input product states $|\varphi_A\rangle|\varphi_B\rangle$ with vanishing mutual coherence. We mainly focus on the nontrivial optimal state $|\psi_3\rangle$ and we generate this state on a quantum photonic platform where qubits are encoded into polarization states of single photons. Our first strategy, illustrated in Fig. 1(a), is based on the application of a suitable probabilistic strictly incoherent quantum operation [9] represented by a single Kraus operator \hat{M} diagonal in the basis of free states,

$$\hat{M} = A|00\rangle\langle 00| + B(|01\rangle\langle 01| + |10\rangle\langle 10|) + C|11\rangle\langle 11|, \quad (9)$$

and satisfying $\hat{M}^\dagger \hat{M} \leq \hat{I}$. This quantum filter transforms a pure input state $|\psi_{\text{in}}\rangle$ onto a pure output state $|\psi_{\text{out}}\rangle = \hat{M}|\psi_{\text{in}}\rangle/\sqrt{P_S}$, with success probability

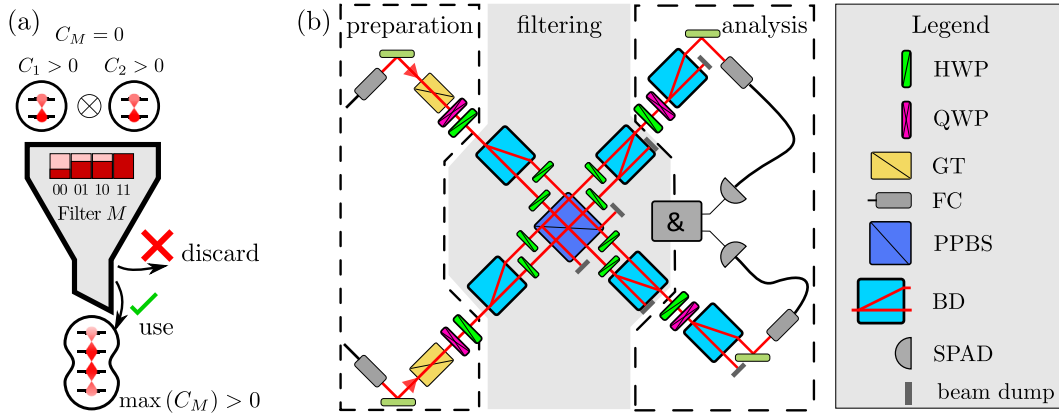


FIG. 1. Mutual coherence generation by a strictly incoherent quantum filter from input product state with $C_M = 0$. Shown are the conceptual scheme of (a) the protocol and (b) the experimental setup. HWP: half-wave plate; QWP: quarter-wave plate; GT: Glan-Taylor polarizer; PPBS: partially polarizing beam splitter; BD: beam-displacing crystal; FC: fiber coupler; and SPAD: single-photon avalanche detector [27].

$P_S = \langle \psi_{\text{in}} | \hat{M}^\dagger \hat{M} | \psi_{\text{in}} \rangle$. Choosing a symmetric product input state,

$$|\psi_{\text{in}}\rangle = (\sqrt{p}|1\rangle + \sqrt{1-p}|0\rangle)^{\otimes 2}, \quad (10)$$

the optimal state $|\psi_3\rangle$ can be obtained by a filter that completely eliminates the state $|00\rangle$, $A = 0$, and

$$\begin{aligned} \hat{M}_- &= q(|01\rangle\langle 01| + |10\rangle\langle 10| + |11\rangle\langle 11|), & p \leq p_{\text{th}}, \\ \hat{M}_+ &= |01\rangle\langle 01| + |10\rangle\langle 10| + q^{-1}|11\rangle\langle 11|, & p > p_{\text{th}}. \end{aligned} \quad (11)$$

Here, $p_{\text{th}} = 2c^2/(1+c^2)$ and $q^2 = p(1-p_{\text{th}})/[p_{\text{th}}(1-p)]$.

In our experiment, time-correlated photon pairs are generated in the process of spontaneous parametric down-conversion in a nonlinear crystal pumped by a cw laser diode [26] and guided to the main setup depicted in Fig. 1(b). Initially, one photon is polarized vertically and the other horizontally and we associate the H/V basis with the computational basis. Polarization states of single photons are manipulated by a combination of quarter- and half-wave plates. The quantum filter \hat{M} is implemented by two-photon interference in a suitably designed, inherently stable multimode interferometer [14,27] composed of calcite beam displacers, a partially polarizing beam splitter, and wave plates. Parameters of the filter are determined by the angular positions of wave plates neighboring the central PPBS. Successful filtering is heralded by the presence of a single photon at each output port of the filter, similarly to linear optical quantum gates operating in the coincidence basis. With our scheme, we can directly implement the quantum filters \hat{M}_- . This is not a significant restriction because, for $p > p_{\text{th}}$, the filter \hat{M}_+ could be obtained as a combination of easily implementable local single-qubit amplitude attenuations $|0\rangle\langle 0| + q^{-1}|1\rangle\langle 1|$ and an accessible filter $\hat{M}_0 = |01\rangle\langle 01| + |10\rangle\langle 10| + |11\rangle\langle 11|$.

IV. EXPERIMENTAL RESULTS

We have applied the quantum filters to a range of input states (10). For $p > p_{\text{th}}$, we have employed the filter \hat{M}_0 , while for $p \leq p_{\text{th}}$, we have applied the optimal filter \hat{M}_- specified in

Eq. (11). The output two-qubit states were comprehensively characterized by quantum state tomography based on the maximum-likelihood reconstruction algorithm. The optical elements in our setup introduce additional single-qubit local phase shifts. These phase shifts do not modify the coherence properties of the state and were compensated in data processing by suitable local single-qubit unitaries, $\exp(i\theta_A \delta_{Z,A}) \otimes \exp(i\theta_B \delta_{Z,B})$, applied to the reconstructed density matrix. The experimentally generated state for $p = 0.125$ is plotted in Fig. 2(c) and the dependence of C_M on p is displayed in Fig. 2(d). Parameters characterizing the prepared state plotted in Fig. 2(c) are summarized in Table I, which displays state fidelity F with the ideal target state, state purity $\mathcal{P} = \text{Tr}[\hat{\rho}^2]$, mutual coherence C_M , and the residual population p_{00} of state $|00\rangle$.

The observed mutual coherence $C_M = 0.78(2)$ is significantly lower than the theoretical expectation $C_M(\psi_3) \approx 1.1$, which is mainly caused by imperfect filtering that leaves some residual population in state $|00\rangle$ [see Fig. 2(e)], as well as residual coherence between this state and the other basis states [see Figs. 2(c) and 2(e)]. This leads to higher local coherences and, consequently, the mutual coherence is reduced. As illustrated in Fig. 2(a), the state $|00\rangle$ is initially dominantly populated, which makes the complete elimination of this state particularly experimentally challenging and sensitive to imperfections. To further confirm the origin of the experimentally observed suboptimal value of C_M , we have artificially eliminated the population of $|00\rangle$ in the reconstructed density matrices and renormalized them. The orange crosses in Fig. 2(d) show that the resulting mutual coherence is close to the theoretical prediction.

For comparison, we have also pursued an alternative preparation strategy based on unitary transformation of a suitably chosen asymmetric input product state,

$$|\psi_{\text{in}}\rangle = [\cos(x)|0\rangle + \sin(x)|1\rangle] \otimes [\cos(y)|0\rangle + \sin(y)|1\rangle],$$

where

$$\cos(x) = \sqrt{\frac{1-c^2}{2}}, \quad \sin(2y) = \sqrt{\frac{1-c^2}{1+c^2}}.$$

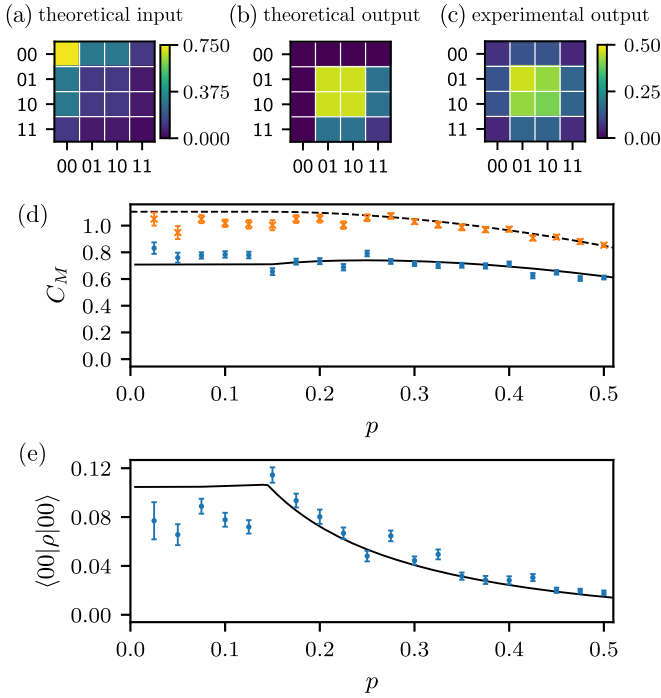


FIG. 2. Generation of mutual coherence from a product two-qubit state. As an example, we plot the real parts of the density matrices of (a) the theoretical input product state with $p = p_{th}$, (b) the corresponding theoretical output state $|\psi_3\rangle$ obtained after application of the filter \hat{M}_- , and (c) the actual experimental output state. The imaginary parts of the theoretical density matrices vanish. We also display the dependence of the mutual coherence of the output state on (d) the input state excitation probability p and (e) the residual population of the unwanted level $|00\rangle$. Blue dots represent experimental data, and the orange crosses in (d) are experimental data after numerical elimination of the level $|00\rangle$ by filter $\hat{M}_0 = \hat{I} - |00\rangle\langle 00|$. Solid lines indicate predictions of a theoretical model of the setup, and the dashed line is the ideal theoretical dependence for a perfect setup. The employed quantum filters are specified in the main text.

This state can be transformed to the state (8) by a sequence of the maximally entangling quantum CZ gate, $\hat{U}_{CZ} = \exp(i\pi|11\rangle\langle 11|)$, followed by local unitary operation $\hat{V}_B = \exp[i(\pi/2 - y)\hat{\sigma}_Y]$ on qubit B , where $\hat{\sigma}_Y = i|0\rangle\langle 1| - i|1\rangle\langle 0|$. We have configured our setup to realize the quantum CZ gate [28–30] which corresponds to the choice $A = B = 1$ and $C = -1$ in Eq. (9). The local unitary operation \hat{V}_B was implemented with a half-wave plate. We have experimentally

TABLE I. Fidelity, purity, mutual coherence, and population of state $|00\rangle$ are displayed for two experimentally generated states $|\psi_3\rangle$ and also state $|\psi_4\rangle$. The experimental uncertainties specified in parentheses represent one standard deviation. The first column indicates how the output state was prepared from a suitable input product state.

Preparation	D	F	\mathcal{P}	C_M	p_{00}
\hat{M}_-	3	0.914(7)	0.92(1)	0.78(2)	0.072(5)
$\hat{V}_B\hat{U}_{CZ}$	3	0.935(6)	0.93(1)	1.18(2)	0.035(3)
\hat{U}_{CZ}	4	0.95(1)	0.92(2)	1.70(6)	–

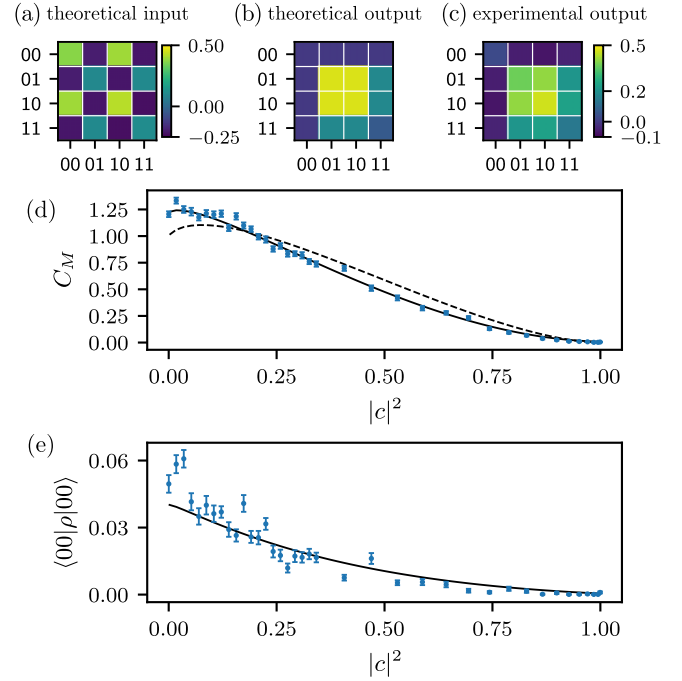


FIG. 3. Generation of the two-qubit states (8) by unitary operations. As an example, we plot the real parts of the density matrices of (a) a theoretical asymmetric input product state for $c = 0.277$, (b) the corresponding theoretical output state obtained by application of CZ gate \hat{U}_{CZ} and local unitary operation \hat{V}_B , and (c) the actual output experimental state prepared with nominal $c = 0.264$. The imaginary parts of the theoretical density matrices vanish. Also shown is (d) the dependence of the mutual coherence of the output state on $|c|^2$ and (e) the residual population of level $|00\rangle$ in the experimentally prepared states. Blue dots represent experimental data, the solid lines indicate predictions of a theoretical model of the setup, and the dashed line shows the ideal theoretical dependence.

probed the generation of the whole single-parametric class of states (8) with $0 < c < 1$.

The experimental results are displayed in Fig. 3. As an illustration, we present in Fig. 3(c) the reconstructed experimentally generated state for nominal target value $c = 0.264$, which has the largest fidelity among all generated states with the target state $|\psi_3\rangle$. Note that the actual parameters of the generated states slightly differ from the nominal theoretical values and the presented experimental state is closest to the optimal state $|\psi_3\rangle$ among the whole set of prepared states. In comparison to the filter-based preparation, the purity and fidelity of the state prepared by unitary operations is higher and the residual population of the state $|00\rangle$ is reduced to 0.035(4); see Table I. The mutual coherence $C_M = 1.18(3)$ slightly exceeds the maximum achievable by the superposition of three basis states $|jk\rangle$. The experimental imperfections in this case thus lead to a slight increase of the mutual coherence. The suppression of the state $|00\rangle$ is generally better than in the filter-based scheme, as illustrated in Fig. 3(d). Our ability to suppress the population of state $|00\rangle$ is mainly limited by imperfect two-photon interference due to the partial distinguishability of the two photons and by the precision of retardance and rotation of wave plates. In order to quantify the effect of wave-plate settings, we numerically search for

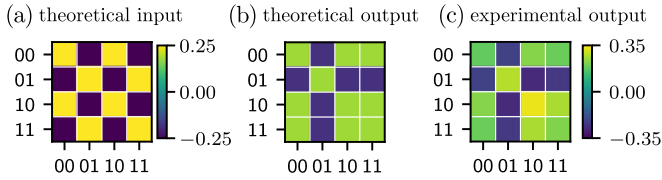


FIG. 4. Generation of the optimal state $|\psi_4\rangle$ with quantum CZ gate. Shown are the real parts of the density matrices of (a) the theoretical input symmetric product state for $p = 0.5$, (b) the theoretical maximally entangled output state $|\psi_4\rangle$, and (c) the experimentally prepared state. The imaginary parts of the theoretical density matrices vanish, and the imaginary parts of the matrix elements of the experimental state in (c) are smaller than 0.011.

optimal local single-qubit unitary operations that minimize the population of state $|00\rangle$, while they keep C_M above a chosen threshold of 1.05. After we apply the optimal single-qubit unitaries to the reconstructed state, the population of $|11\rangle$ drops to $p_{00} = 0.012(2)$, while the mutual coherence of the state remains high, $C_M = 1.05(3)$.

To complete our analysis of the preparation of states that maximize the mutual quantum coherence, we have utilized the quantum CZ gate to generate the optimal maximally entangled state $|\psi_4\rangle$ from input product states $|\pm\rangle|\pm\rangle$, where $|\pm\rangle = (|0\rangle \pm |1\rangle)/\sqrt{2}$. Note that for unbalanced input states, one could first apply local quantum filters to balance the amplitudes of $|0\rangle$ and $|1\rangle$ and then use the quantum CZ gate. Representative results for input $|+\rangle|-\rangle$ are plotted in Fig. 4. The purity and fidelity of the generated state read $F = 0.95(1)$ and $\mathcal{P} = 0.92(2)$ and are, for comparison, also listed in Table I. The mutual coherence of the state is close to the theoretical maximum, $C_M = 1.70(6)$. The state $|\psi_4\rangle$ simultaneously also maximizes the ordinary global coherence and, for the experimentally prepared state, we get $C = 1.71(6)$. On the other hand, the local coherences practically vanish because the state is maximally entangled and each subsystem is locally in a maximally mixed state. The prepared state is not perfectly pure due to the residual distinguishability of the two photons and the amplitudes of the states $|jk\rangle$ are not perfectly balanced due to various experimental imperfections, which explains why the experimental mutual coherence is less than the theoretical maximum, $C_M = 2$.

The observed purities and fidelities of the generated two-qubit states are consistent with high purities and fidelities of the quantum operations that were used for their preparation. Note that the input product states for preparation of the optimal states $|\psi_N\rangle$ are superposition states which are typically more sensitive to gate imperfections than the basis states $|jk\rangle$. We have characterized the experimental two-qubit quantum filters and gates by full quantum process tomography. Each two-qubit quantum operation \mathcal{E} is described by its Choi matrix χ that can be obtained by applying \mathcal{E} to one part of a four-qubit maximally entangled state. This Choi-Jamiołkowski isomorphism between quantum operations and states allows us to conveniently define the purity and fidelity

TABLE II. Purity and fidelity of selected experimental two-qubit quantum operations. The last four columns display the experimentally determined filter parameters that most closely match the experimental data. Since the experimentally implemented operations are not exactly symmetric, we specify separate parameters B_{01} and B_{10} for states $|01\rangle$ and $|10\rangle$.

Gate	\mathcal{P}	F	$ A $	$ B_{01} $	$ B_{10} $	$ C $
\hat{I}	0.985(1)	0.9912(5)	0.950	0.901	1.000	0.957
\hat{M}_0	0.963(5)	0.965(3)	0.243	0.949	1.000	0.928
\hat{U}_{CZ}	0.927(6)	0.957(3)	0.801	0.951	1.000	0.881

of the quantum operation by straightforward extension of the definitions for quantum states. In Table II, we summarize the experimental results for the filter \hat{M}_0 and the unitary gate \hat{U}_{CZ} . For reference, we also provide results for the two-qubit identity operation \hat{I} . The achieved fidelities are fully comparable to the highest fidelities of linear optical two-qubit quantum gates and operations reported in the literature [31–34].

V. CONCLUSIONS

In this paper, we have studied the mutual coherence in various subspaces of the Hilbert space of a pair of qubits. First, we have theoretically investigated and characterized states maximizing mutual coherence in the subspaces of dimension $\{2, 3, 4\}$. In our study, we quantify the coherence by the relative entropy of coherence. For this coherence measure, our results reveal the nontrivial structure of the optimal states in dimension 3, whereas in even-dimensional subspaces, the states show high symmetry. Subsequently, we have generated the optimal states in a linear-optical proof-of-principle experiment. We have realized strictly incoherent two-qubit quantum filters capable of transforming an initial product state of two qubits with a certain amount of local coherence into a state maximizing the mutual coherence. Furthermore, we have also prepared the optimal states via a sequence of unitary operations that involves single-qubit transformation outside the class of strictly incoherent operations. Our experimental results confirm the complex behavior of mutual coherence in the three-dimensional subspace and show that the mutual coherence as a nonlinear quantity is highly sensitive to imperfections. Our results pave the way for further investigations of the properties of mutual coherence in nontrivial subspaces of composite Hilbert spaces.

ACKNOWLEDGMENTS

R.S., M.M., J.F., and M.K. acknowledge support by the Czech Science Foundation under Grant No. 19-19189S. N.H. and R.S. acknowledge support from Palacký University under Grants No. IGA-PrF-2021-006 and No. IGA-PrF-2022-005. R.F. acknowledges support by the Czech Science Foundation under Grant No. 20-16577S.

[1] T. Baumgratz, M. Cramer, and M. B. Plenio, Quantifying Coherence, *Phys. Rev. Lett.* **113**, 140401 (2014).

[2] A. Winter and D. Yang, Operational Resource Theory of Coherence, *Phys. Rev. Lett.* **116**, 120404 (2016).

- [3] A. Streltsov, G. Adesso, and M. B. Plenio, Colloquium: Quantum coherence as a resource, *Rev. Mod. Phys.* **89**, 041003 (2017).
- [4] E. Chitambar and G. Gour, Quantum resource theories, *Rev. Mod. Phys.* **91**, 025001 (2019).
- [5] M. A. Nielsen and I. L. Chuang, *Quantum Computation and Quantum Information* (Cambridge University Press, Cambridge, 2000).
- [6] C. L. Degen, F. Reinhard, and P. Cappellaro, Quantum sensing, *Rev. Mod. Phys.* **89**, 035002 (2017).
- [7] E. Chitambar, A. Streltsov, S. Rana, M. N. Bera, G. Adesso, and M. Lewenstein, Assisted Distillation of Quantum Coherence, *Phys. Rev. Lett.* **116**, 070402 (2016).
- [8] B. Regula, K. Fang, X. Wang, and G. Adesso, One-Shot Coherence Distillation, *Phys. Rev. Lett.* **121**, 010401 (2018).
- [9] K. Fang, X. Wang, L. Lami, B. Regula, and G. Adesso, Probabilistic Distillation of Quantum Coherence, *Phys. Rev. Lett.* **121**, 070404 (2018).
- [10] C. L. Liu and D. L. Zhou, Deterministic Coherence Distillation, *Phys. Rev. Lett.* **123**, 070402 (2019).
- [11] K.-D. Wu, Z. Hou, H.-S. Zhong, Y. Yuan, G.-Y. Xiang, C.-F. Li, and G.-C. Guo, Experimentally obtaining maximal coherence via assisted distillation process, *Optica* **4**, 454 (2017).
- [12] K.-D. Wu, Z. Hou, Y.-Y. Zhao, G.-Y. Xiang, C.-F. Li, G.-C. Guo, J. Ma, Q.-Y. He, J. Thompson, and M. Gu, Experimental Cyclic Interconversion between Coherence and Quantum Correlations, *Phys. Rev. Lett.* **121**, 050401 (2018).
- [13] M. Gumberidze, M. Kolář, and R. Filip, Measurement induced synthesis of coherent quantum batteries, *Sci. Rep.* **9**, 19628 (2019).
- [14] J. Fiurášek, R. Stárek, and M. Mičuda, Optimal implementation of two-qubit linear-optical quantum filters, *Phys. Rev. A* **103**, 062408 (2021).
- [15] Z. Xi, Y. Li, and H. Fan, Quantum coherence and correlations in quantum system, *Sci. Rep.* **5**, 10922 (2015).
- [16] Y. Guo and S. Goswami, Discordlike correlation of bipartite coherence, *Phys. Rev. A* **95**, 062340 (2017).
- [17] X.-L. Wang, Q.-L. Yue, C.-H. Yu, F. Gao, and S.-J. Qin, Relating quantum coherence and correlations with entropy-based measures, *Sci. Rep.* **7**, 12122 (2017).
- [18] K. C. Tan and H. Jeong, Entanglement as the Symmetric Portion of Correlated Coherence, *Phys. Rev. Lett.* **121**, 220401 (2018).
- [19] M. Gumberidze, M. Kolář, and R. Filip, Pairwise-measurement-induced synthesis of quantum coherence, *Phys. Rev. A* **105**, 012401 (2022).
- [20] Q. Zhao, Y. Liu, X. Yuan, E. Chitambar, and X. Ma, One-Shot Coherence Dilution, *Phys. Rev. Lett.* **120**, 070403 (2018).
- [21] P. Kammerlander and J. Anders, Coherence and measurement in quantum thermodynamics, *Sci. Rep.* **6**, 22174 (2016).
- [22] T. Kraft and M. Piani, Genuine correlated coherence, *J. Phys. A: Math. Theor.* **51**, 414013 (2018).
- [23] Y. Yao, X. Xiao, L. Ge, and C. P. Sun, Quantum coherence in multipartite systems, *Phys. Rev. A* **92**, 022112 (2015).
- [24] J. Ma, B. Yadin, D. Girolami, V. Vedral, and M. Gu, Converting Coherence to Quantum Correlations, *Phys. Rev. Lett.* **116**, 160407 (2016).
- [25] K. C. Tan, H. Kwon, C.-Y. Park, and H. Jeong, Unified view of quantum correlations and quantum coherence, *Phys. Rev. A* **94**, 022329 (2016); **96**, 069905(E) (2017).
- [26] M. Ježek, I. Straka, M. Mičuda, M. Dušek, J. Fiurášek, and R. Filip, Experimental Test of the Quantum Non-Gaussian Character of a Heralded Single-Photon State, *Phys. Rev. Lett.* **107**, 213602 (2011).
- [27] R. Stárek, M. Mičuda, M. Kolář, R. Filip, and J. Fiurášek, Experimental demonstration of optimal probabilistic enhancement of quantum coherence, *Quantum Sci. Technol.* **6**, 045010 (2021).
- [28] N. Kiesel, C. Schmid, U. Weber, R. Ursin, and H. Weinfurter, Linear Optics Controlled-Phase Gate Made Simple, *Phys. Rev. Lett.* **95**, 210505 (2005).
- [29] N. K. Langford, T. J. Weinhold, R. Prevedel, K. J. Resch, A. Gilchrist, J. L. O'Brien, G. J. Pryde, and A. G. White, Demonstration of a Simple Entangling Optical Gate and Its Use in Bell-State Analysis, *Phys. Rev. Lett.* **95**, 210504 (2005).
- [30] R. Okamoto, H. F. Hofmann, S. Takeuchi, and K. Sasaki, Demonstration of an Optical Quantum Controlled-NOT Gate without Path Interference, *Phys. Rev. Lett.* **95**, 210506 (2005).
- [31] B. P. Lanyon, M. Barbieri, M. P. Almeida, T. Jennewein, T. C. Ralph, K. J. Resch, G. J. Pryde, J. L. O'Brien, A. Gilchrist, and A. G. White, Simplifying quantum logic using higher-dimensional Hilbert spaces, *Nat. Phys.* **5**, 134 (2009).
- [32] H. W. Li, S. Przeslak, A. O. Niskanen, J. C. F. Matthews, A. Politi, P. Shadbolt, A. Laing, M. Lobino, M. G. Thompson, and J. L. O'Brien, Reconfigurable controlled two-qubit operation on a quantum photonic chip, *New J. Phys.* **13**, 115009 (2011).
- [33] J. Carolan, C. Harrold, C. Sparrow, E. Martín-López, N. J. Russell, J. W. Silverstone, P. J. Shadbolt, N. Matsuda, M. Oguma, M. Itoh, G. D. Marshall, M. G. Thompson, J. C. F. Matthews, T. Hashimoto, J. L. O'Brien, and A. Laing, *Science* **349**, 711 (2015).
- [34] M. Zhang, L. Feng, M. Li, Y. Chen, L. Zhang, D. He, G. Guo, G. Guo, X. Ren, and D. Dai, Supercompact Photonic Quantum Logic Gate on a Silicon Chip, *Phys. Rev. Lett.* **126**, 130501 (2021).